*Texture of Crystalline Solids*
1976, Vol. 2, pp. 95-111


# QUANTITATIVE DETERMINATION OF PREFERRED ORIENTATION BY ENERGY-DISPERSIVE X-RAY DIFFRACTION

L. GERWARD, S. LEHN, and G. CHRISTIANSEN
*Laboratory of Applied Physics III, Building 307, Technical University of Denmark, DK-2800 Lyngby, Denmark*

*(Received February 1, 1976)*

*Abstract:* The use of energy-dispersive X-ray diffraction for quantitative determination of preferred orientations in polycrystalline specimens is analysed. The method is applied to determinations of rolling texture and fibre texture. The adaptability of the method to *in situ* studies is demonstrated by observations of texture changes simultaneous with the deformation of a specimen in a tension test.

## 1. INTRODUCTION

The purpose of the present work is to develop energy-dispersive X-ray diffractometry into a useful tool for quantitative analysis of preferred orientation. Energy-dispersive diffraction, introduced in 1968,[1,2] has some unique advantages compared with standard angle-dispersive diffraction but requires some changes in the analytical procedures generally used.

In energy-dispersive diffraction a beam of polychromatic X-rays is incident on the crystalline specimen. The photon-energy spectrum of the scattered X-rays is measured by a semiconductor detector connected to a multichannel pulse-height analyser. In this way several Bragg reflections are recorded simultaneously. The information obtained with a fixed scattering angle and a fixed specimen orientation is sufficient for the determination of an inverse pole figure. Alternatively, several normal pole figures can be obtained with a fixed scattering angle by varying the specimen orientation.

Laine and Lähteenmäki[3] used an energy-dispersive method to study preferred orientation in splat-cooled cadmium. They used the intensity ratio of the 002 diffraction line and the Cd Kα fluorescence line as a measure of the preferred orientation. Szpunar, Ojanen and Laine[4] showed that the spectrum of diffraction lines can be used for the construction of inverse pole figures. A similar method using neutron diffraction and time-of-flight analysis was proposed by Szpunar, Olés, Buras, Sosnowski and Pietras.[5]

The quantitative determination of rolling texture and fibre texture using energy-dispersive diffraction is developed in the present work. The theoretical formula for the integrated intensity in terms of the photon energy is derived starting with an ideal non-absorbing specimen without texture and then applying various corrections. In particular, the absorption in a real specimen affects the observed intensities to a large extent. This makes it difficult to compare the X-ray patterns for different positions of the specimen. In addition, the absorption is strongly wavelength dependent. This is a complication in energy-dispersive diffraction where a continuous X-ray spectrum is used. The X-ray absorption coefficient for a given specimen may vary by almost two powers of ten within the useful wavelength range.

The determination of inverse pole figures is hampered by problems associated with normalizing the data. In this work it is shown how the normalizing can be improved by optimizing the scattering angle and by separating the intensity contributions of the overlapping diffraction peaks.

The energy-dispersive method is well suited for *in situ* studies on specimens subjected to various controlled environments. This has been demonstrated in a dynamic experiment: changes in the texture of a recrystallized aluminium wire have been observed by energy-dispersive diffraction analysis simultaneous with the deformation of the specimen in a tension test machine.

## 2. ENERGY-DISPERSIVE DIFFRACTOMETRY

Figure 1 shows the principle of energy-dispersive X-ray diffractometry. Using this method the Bragg equation can be written in the following form

$$(Ed)_{hk\ell} \sin \theta_0 = hc/2, \qquad (1)$$

where $E_{hk\ell}$ = X-ray photon energy, $d_{hk\ell}$ = interplanar spacing, $\theta_0$ = fixed Bragg angle, h= Planck's constant and c = velocity of light. For practical purposes it

is convenient to notice that the constant on the right-hand side of Equation (1) equals $hc/2 = 6.199$ keV·Å if E is expressed in keV and d in Å.

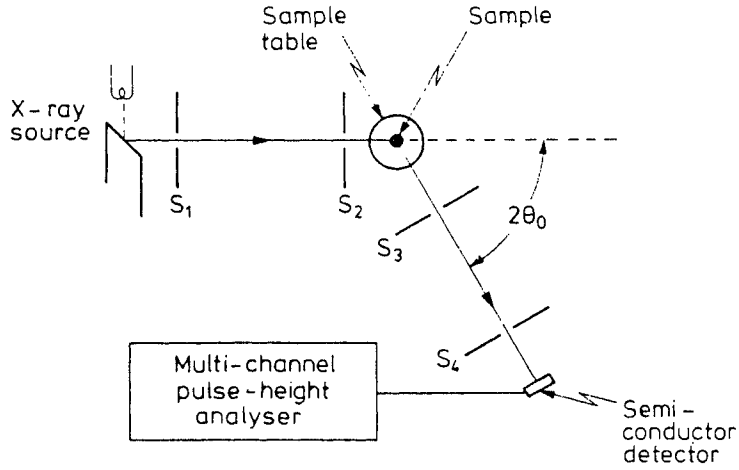


FIGURE 1. Principle of the energy-dispersive X-ray method. $S_1$, $S_2$, $S_3$ and $S_4$ = slits defining the beam paths, $2\theta_0$ = fixed scattering angle.

In this work we have used the continuous X-ray spectrum from a tungsten tube and a Si(Li) detector. A more detailed description of the equipment is given elsewhere.[6] The experimental diffraction peaks have been corrected for the background and fitted to a Gaussian shape in order to calculate the integrated intensities, half widths and peak positions. Using curve fitting it has also been possible to separate diffraction peaks which are partly overlapping.

## 3. INTEGRATED INTENSITIES

For a powder specimen the integrated intensity, i.e., the total diffracted power, in a complete Debye-Scherrer ring using the energy-dispersive method is given by[7]

$$r_e^2 N^2 V [i_0(\lambda)\lambda^4 \; j \; |F|^2]_{hk\ell} \frac{(1+\cos^2 2\theta_0)}{8 \sin \theta_0} \cot \theta_0 \; \Delta\theta_0, \quad (2)$$

where $r_e = 2.82 \times 10^{-13}$ cm = the classical electron radius, N = number of crystal unit cells per unit volume, V = volume of irradiated material, $i_0(\lambda)$ = intensity per unit wavelength range of the incident beam, j = multiplicity factor, F = structure factor and $\Delta\theta_0$ = divergence of the X-ray beam.

Equation (2) has been derived with the assumptions that the orientations of the crystallites are randomly distributed and that absorption and extinction are

negligible.* The subscript hkℓ indicates that the quantities λ, j and F depend on the reflection hkℓ.

Preferred orientations are described by the orientation distribution $p_{hk\ell}(\alpha,\beta)$. This is proportional to the volume fraction of material having normals to a given family of lattice planes (hkℓ) oriented in a small solid angle dΩ in the angular range α to α + dα, β to β + dβ, relative to some fixed directions in the specimen. The orientation distribution is unity for a random specimen.

Absorption is taken into account by multiplying Equation (2) with the absorption factor $A(\lambda, \theta_0, \alpha,\beta)$. In the energy-dispersive method, where the wavelength is variable, the absorption factor depends on the wavelength of the diffracted X-rays as well as on the diffraction geometry.

It is generally very difficult to apply extinction corrections. In the energy-dispersive method it is even more complicated due to the wavelength dependence. In this work we assume that the grain size of the polycrystalline specimen is sufficiently small (of the order of a few μm) so that the extinction can be neglected.

The diffracted intensity is recorded as a function of the photon energy by the semiconductor detector system. It is therefore convenient to express the integrated intensities on the photon energy scale using

$$i_0(E) = \left|\frac{d\lambda}{dE}\right| i_0(\lambda) = (\lambda^2/hc) i_0(\lambda) = (hc/E^2) i_0(\lambda), \quad (3)$$

where $i_0(E)$ = intensity per unit energy range of the incident beam.

Finally, we take into account that the detector records the fraction $D/2\pi\ r \sin 2\theta_0$ (D = height of detector window and r = distance between sample and detector) of the total intensity in the Debye-Scherrer ring.

Inserting the corrections discussed above in Equation (2) one obtains the following expression for the integrated intensity, $I_{hk\ell}$, to be used in the energy-dispersive analysis**:

---

*Furthermore the incident beam is supposed to be unpolarized. Polarization effects may have to be considered for the shortest wavelengths of the incident spectrum.[8]

**Another obvious correction is that due to the spectral response of the detector. However, if the same detector is used throughout the experiments one can regard the intensity $i_0$ as the effective intensity as seen by the detector.

$$I_{hk\ell}=(hc)^3 r_e^2 \frac{D}{r} N^2 V[i_0(E)E^{-2} j|F|^2 A(E,\theta_0,\alpha,\beta)p(\alpha,\beta)]_{hk\ell} \frac{1+\cos^2 2\theta_0}{32\pi \sin^3\theta_0}\Delta\theta \quad (4)$$

Equation (4) may be written more concisely as

$$I_{hk\ell} = C[i_0(E)E^{-2}\ j|F|^2 A(E,\theta_0,\alpha,\beta)p(\alpha,\beta)]_{hk\ell} \quad (5)$$

where C is a constant depending on the diffraction geometry.

## 4. DETERMINATION OF INVERSE POLE FIGURES

In the energy-dispersive method a number of reflections hkℓ are recorded simultaneously in a given diffraction geometry. For example, a wire specimen can be arranged so that the wire axis is parallel to the scattering vector.* In this way lattice planes having normals along the wire axis contribute to the diffracted intensities. The observed diffraction pattern can be directly used for quantitative analysis by the construction of the inverse pole figure according to Harris' method[9] with some modifications due to the use of a continuous X-ray spectrum.

The integrated intensities of the specimen are compared with those of a random specimen. The ratio of the corresponding intensities, corrected for absorption, will be called $x_{hk\ell}$. It follows from Equation (5) that

$$x_{hk\ell} = \left(\frac{I}{I_r}\frac{A_r}{A}\right)_{hk\ell} = \frac{C}{C_r} p_{hk\ell}\ , \quad (6)$$

where the subscript r denotes the random specimen.

The orientation distribution for a given family of lattice planes (hkℓ) is normalized in real space by

$$\frac{1}{2\pi}\int\int p_{hk\ell}(\alpha,\beta)\ d\Omega = 1, \quad h,k,\ell = \text{const.}, \quad (7)$$

---

*The scattering vector is parallel to $\underset{\sim}{u} - \underset{\sim}{u}_0$, where $\underset{\sim}{u}$ = unit vector in the direction of the scattered beam and $\underset{\sim}{u}_0$ = unit vector in the direction of the incident beam.

where the integration is performed over all orientations relative to the specimen. In reciprocal space one has to resort to an approximate normalization by assuming that for a large number of reflections in a given diffraction geometry one has

$$\frac{1}{n} \sum_{hk\ell} p_{hk\ell}(\alpha,\beta) \simeq 1, \quad \alpha,\beta = \text{const.} \tag{8}$$

where n = number of p-values considered. It should be noted that only one p-value is counted when several orders of reflection from a particular family of lattice planes are observed.

The p-values associated with the direction parallel to the scattering vector can now be obtained using Equation (6) and the normalizing condition, Equation (8):

$$p_{hk\ell} = x_{hk\ell} \frac{n}{\sum_{h'k'\ell'} x_{h'k'\ell'}} \tag{9}$$

In structures of high symmetry it often occurs that different families of lattice planes have the same interplanar spacing. The corresponding diffraction lines appear at the same photon energy according to Equation (1). In many cases the intensity contributions from each of the reflections can be separated because the p-value for one family of lattice planes is known from another order of reflection.

Consider two reflections, $h_1k_1\ell_1$ and $h_2k_2\ell_2$, which coincide in the diffraction pattern. According to Equation (5) the measured integrated intensity is given by*

$$I_{1,2} = C[i_0(E)E^{-2}|F|^2 A]_{1,2} \times (j_1p_1 + j_2p_2). \tag{10}$$

For the random specimen one has a similar expression but with $p_1 = p_2 = 1$. The ratio of the intensities from the specimen and the random specimen, corrected for the absorption is then

---

*Here we assume that the two reflections have the same structure factor. In non-centrosymmetric crystals the structure factors may differ due to dispersion effects and Equation (10) should be modified.

$$x_{1,2} = \left(\frac{I}{I_r}\frac{A_r}{A}\right)_{1,2} = \frac{C}{C_r}\frac{j_1p_1 + j_2p_2}{j_1 + j_2} = \frac{j_1x_1 + j_2x_2}{j_1 + j_2}, \quad (11)$$

where $x_1$ and $x_2$ are the ratios, which would have been observed if the reflections had not coincided, If $x_1$ is known from another order of reflection then $x_2$ can be calculated from Equation (11). Examples are given in the following sections.

## 5. ROLLING TEXTURE

Determination of rolling texture has been exemplified using a cold-rolled thin foil of α-iron (purity better than 99.9%). The thickness of the foil has been determined as 15.6 μm. Foils of this kind are supplied as X-ray filters in sheets of 20 mm x 170 mm in size by Johnson & Matthey Chemicals Ltd., London. Photographically recorded Debye-Scherrer rings were used to control the grain size.

Figure 2 shows the diffraction pattern for an iron powder used as the random specimen. Figures 2b and 2c show the corresponding patterns for the iron sheet oriented with the rolling direction parallel to the scatering vector (Figure 2b) and with the surface normal parallel to the scattering vector (Figure 2c). The qualitative features of the texture can be found immediately by visual inspection of the spectra. Notice for example that the 022 reflection is very strong in Figure 2b but almost absent in Figure 2c.

The 011 and 002 diffraction lines have been omitted because they overlap the tungsten L-lines of the X-ray spectrum. However, $p_{011}$ can be determined from the 022 and 044 reflections, which are present in the spectrum. In the same way $p_{001}$ can be determined from the 004 reflection. The contributions of the 033/114 and the 006/244 peaks can be separated according to the method described in Section 4. The reflections up to and including 136 have been used. In this way the p-values can be normalized using 13 points in the inverse pole figure.

It has been found that a scattering angle about $2\theta_0 = 50$ deg is the best choice in the present case. At this angle the largest number of useful diffraction peaks is situated within the observable energy range.

Absorption factors for a specimen in the shape of a sheet large enough to intercept the entire incident beam are given in the International Tables for X-ray Crystallography[10] and in many textbooks on X-ray crystallography.

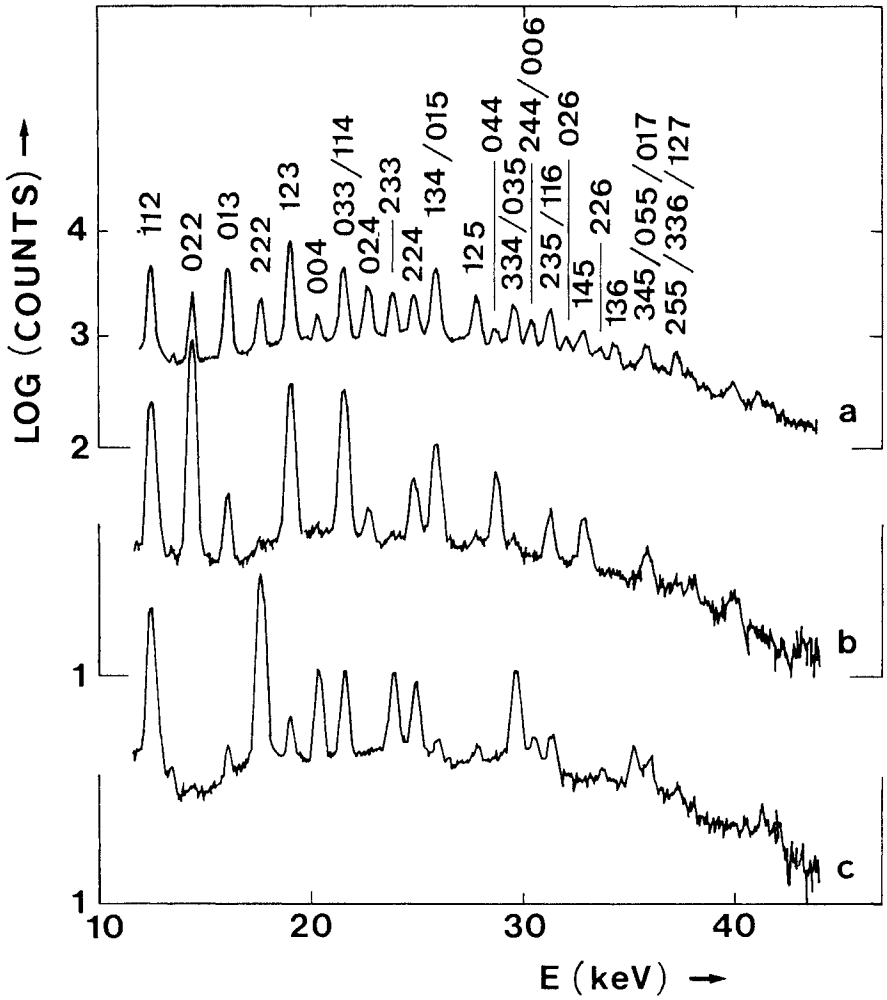


FIGURE 2. Energy-dispersive X-ray diffraction patterns of iron. $2\theta_0 = 50°$. (a) Random specimen (powder). (b) Rolled sheet, rolling direction parallel to scattering vector. (c) Rolled sheet, surface normal parallel to scattering vector. Notice the presence of a strong texture.

The photon energy dependence of the X-ray absorption coefficient has been taken into account using the relation

$$\mu(E)/\rho = k\, E^{-m} , \qquad (12)$$

where $\mu(E)$ = linear absorption coefficient, $\rho$ = density of mass and k and m are constants as long as no absorption edge is included in the energy range.

Linear regression analysis of the absorption data given in the International Tables of X-Ray Crystallography (Vol. IV)[10] has given $k = 1.321 \times 10^4$, $m = 2.820$ ($\mu/\rho$ in units of $cm^2/g$) and the coefficient of determination $r^2 = 0.99998$ for $E < 7.11$ keV (iron K-absorption edge) and $k = 9.019 \times 10^4$, $m = 2.728$ and $r^2 = 0.99991$ for $E > 7.11$ keV.

Figures 3a and 3b show the inverse pole figures in the rolling direction and the normal direction, respectively. The highest probabilities are observed for {111} planes parallel to the sheet surface and <110> directions parallel to the rolling direction but other texture systems can also be observed in the pole figures.

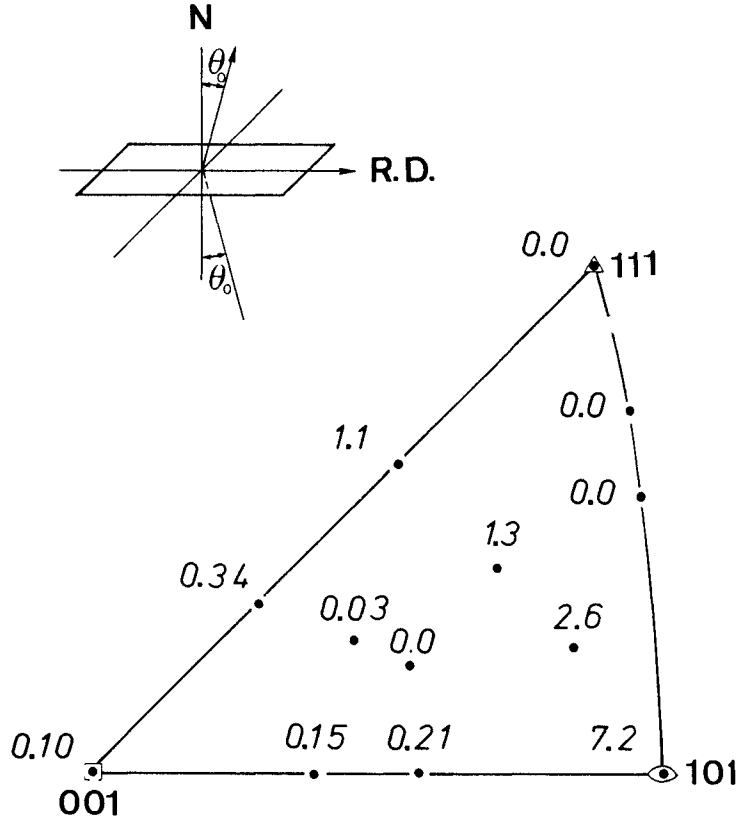


FIGURE 3a. Inverse pole figure of iron. Rolling direction.

The reproducibility of the p-values has been estimated in two ways: (1) The p-values determined from different orders of reflections available in the same diffraction pattern have been found to agree within 10%; (2) Using the diffraction patterns recorded at three different scattering angles and normalizing them with

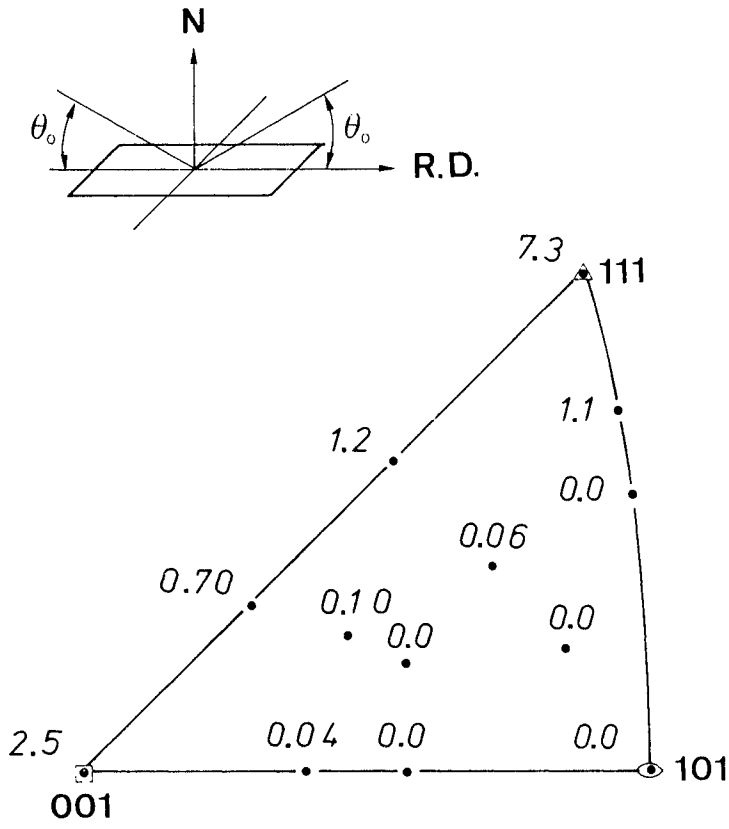


FIGURE 3b. Inverse pole figure of iron. Normal direction.

the same number of reflections we find that the corresponding p-values agree within 15%.

## 6. FIBRE TEXTURE

The determination of inverse pole figures are of particular value in the analysis of axisymmetric specimens. Figure 4 shows a diffraction pattern from an aluminium wire. The wire axis is placed parallel to the scattering vector. It is obvious that the wire has a strong [111] texture. The very characteristic features are that the 002 reflection has almost disappeared from the wire sample, and that the relative intensities of the 113 and 222 peaks are reversed compared with the random specimen.

For the random specimen a capillary filled with aluminium powder was chosen. Absorption factors for the random specimen and the wire oriented with the wire axis perpendicular to the scattering vector are given in the

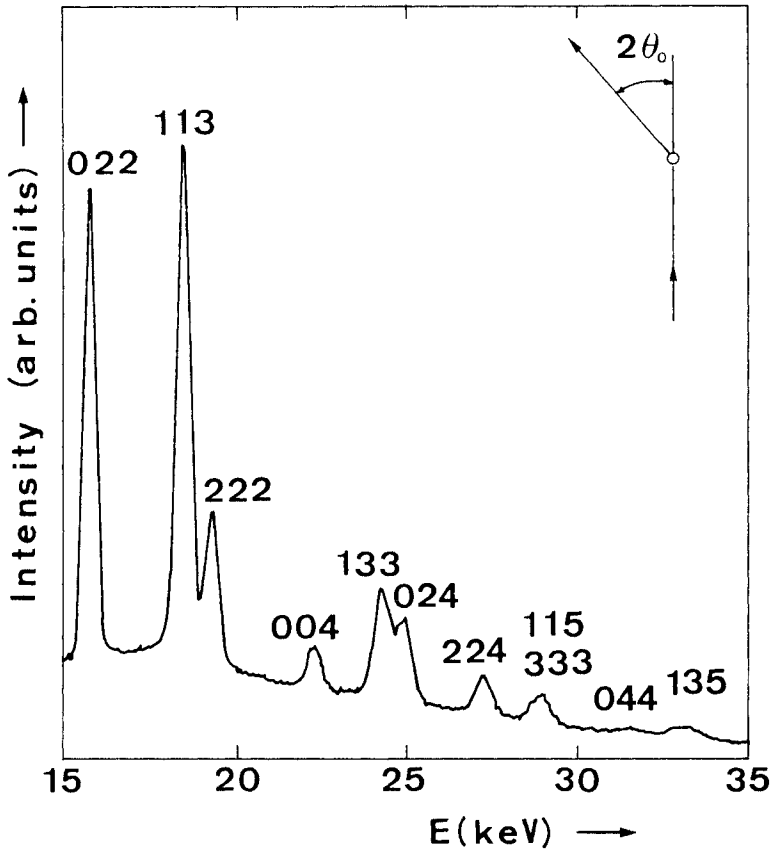


FIGURE 4a. Energy-dispersive X-ray diffraction pattern of aluminum. $2\theta_0 = 32°$. Random specimen (powder).

International Tables for X-Ray Crystallography.[10]

The absorption factor for a wire specimen oriented with its axis parallel to the scattering vector has been calculated in this work using the definition of A: The X-rays reflected by the specimen are reduced by a factor

$$A = \frac{1}{V} \cdot \int \exp[-\mu(p + q)]dV \ , \qquad (13)$$

where V = volume of irradiated material, p and q = lengths of the paths of the incident and reflected beams, respectively, in the crystal.

Figure 5 shows the diffraction geometry. It follows from the symmetry that the sum of the beam paths are the chord of an ellipse. Equation (13) can then be written

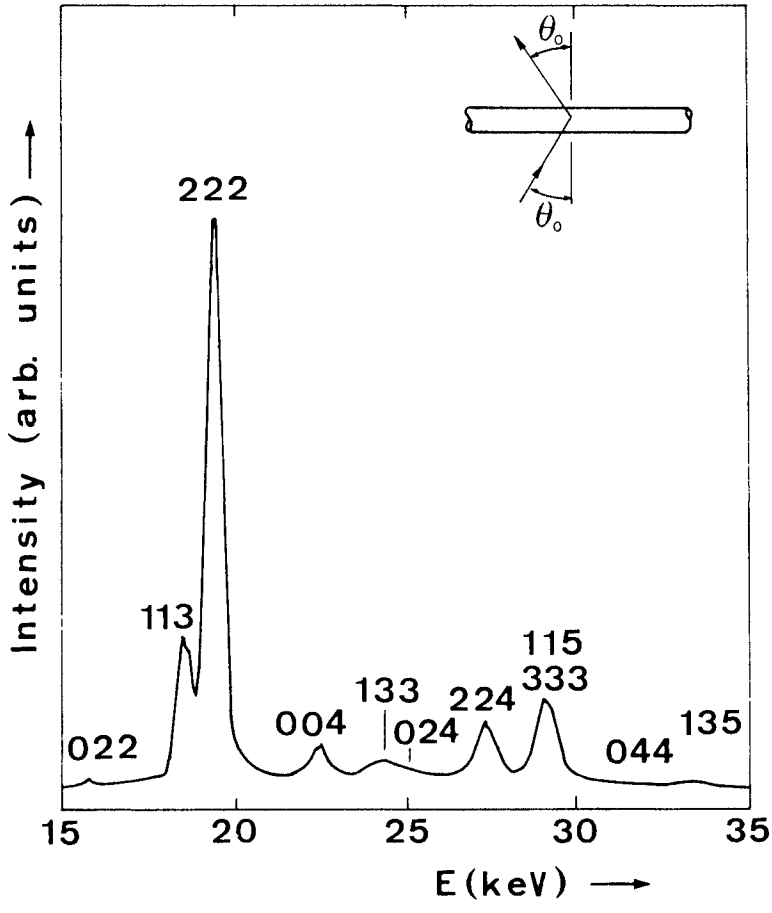


FIGURE 4b. Energy-dispersive X-ray diffraction pattern of aluminium. $2\theta_0 = 32°$. Wire, wire axis parallel to scattering vector.

$$A = \frac{2}{\pi R} \int_{-R}^{R} \sqrt{1 - y^2/R^2}\, \exp\left(-\frac{2\mu R}{\cos\theta_0} \sqrt{1 - y^2/R^2}\right) dy, \qquad (14)$$

where R = radius of the wire. Equation (14) has been solved by numerical integration.

The linear absorption coefficient for the photon energy of each of the diffraction lines was calculated according to Equation (12) using $k = 2.266 \times 10^4$, $m = 2.937$ ($\mu/\rho$ in $cm^2/g$) and $r^2 = 0.99996$.

The inverse pole figure for the direction parallel to the wire axis is shown in Figure 6. The 333/115 contributions have been separated according to the method described in Section 4. The p-values have been normalized using 9 points.

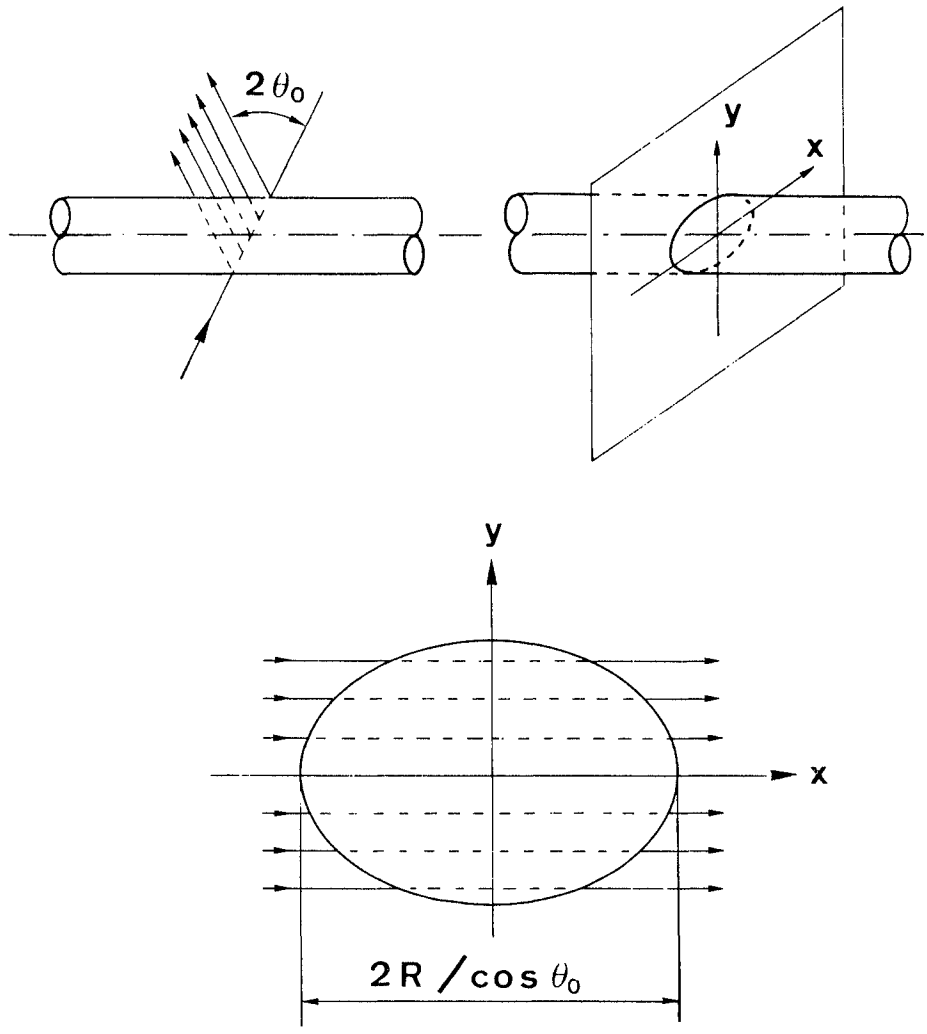


FIGURE 5. Diffraction geometry for calculating the absorption factor of a wire specimen. Wire axis parallel to scattering vector. (Notation, see text.)

## 7. A DYNAMIC EXPERIMENT

The advantages of a fixed scattering angle and a rapid data acquisition make the energy-dispersive method suitable for texture studies in dynamic experiments. This has been demonstrated in a tension test where changes in the texture are observed simultaneously with the deformation of the specimen.

Figure 7 shows the experimental arrangement. The specimen is an aluminium wire of the same kind as the one used in Section 5. The X-ray tube and the detector

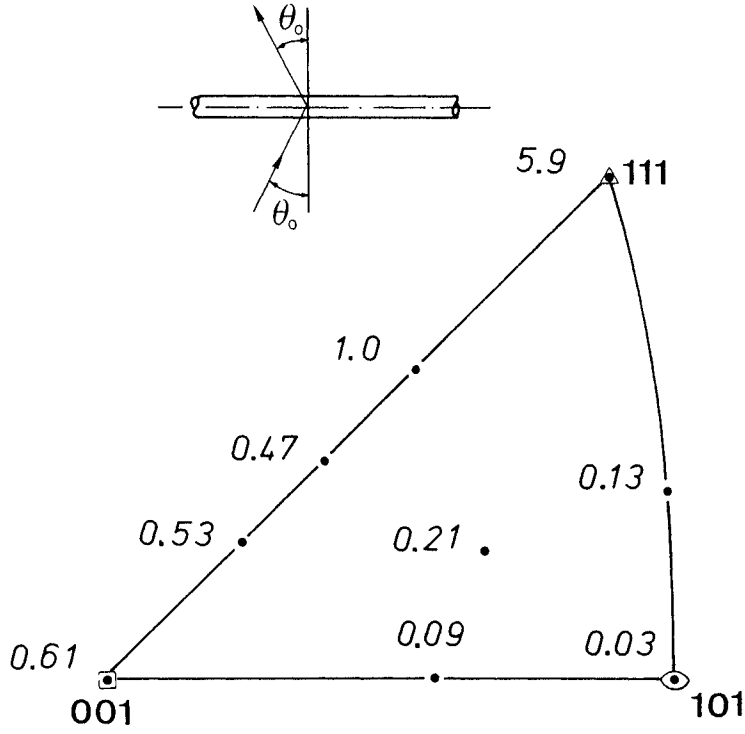


FIGURE 6. Inverse pole figure of aluminium wire. Direction parallel to wire axis.

were inclined about 15° with respect to the vertical and placed close to an Instron Model 1026 tension test machine. The wire specimen was mounted vertically and loaded in steps of about 0.5 kg until break occurred. After each step a diffraction pattern was recorded in a counting time of 100 s.

The texture of the wire as it was received from the manufacturer appeared to be insensitive to the deformation. No changes in the diffraction patterns were observed until break occurred. Therefore a new series of experiments was performed with samples, which were heat treated at 550°C before the tension test.

The heat treatment resulted in a texture which was sensitive to the deformation. Figures 8a to 8c show some diffraction patterns recorded during a tension test. At about one half of the maximum load one observes a gradual decrease of the 222 peak and a corresponding increase of the 133/024 peak (the two lines are not resolved in the spectra).

The experiments have shown that the energy-dispersive method can rather easily be adapted to dynamic studies. In this way, the method could be used for line control of the texture in production processes, such as

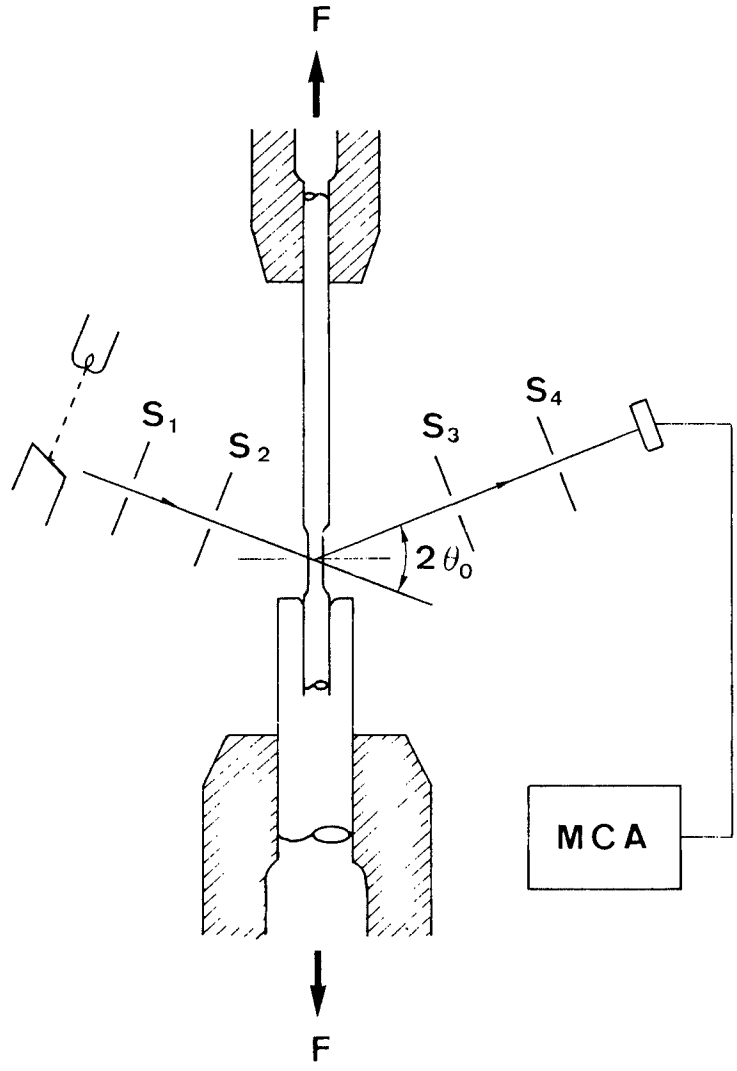


FIGURE 7. Experimental arrangement (schematic) for X-ray diffraction analysis simultaneous with tension test of wire specimen. F = applied force, MCA = multichannel pulse-height analyser.

the forming of a wire or a sheet. With the X-ray tube and detector mounted close to a heat chamber the development of recrystallization texture could be followed in a similar way as a function of temperature and time.

ACKNOWLEDGMENTS

The work reported here was made possible by a grant from Statens teknisk-videnskabelige Fond. This financial

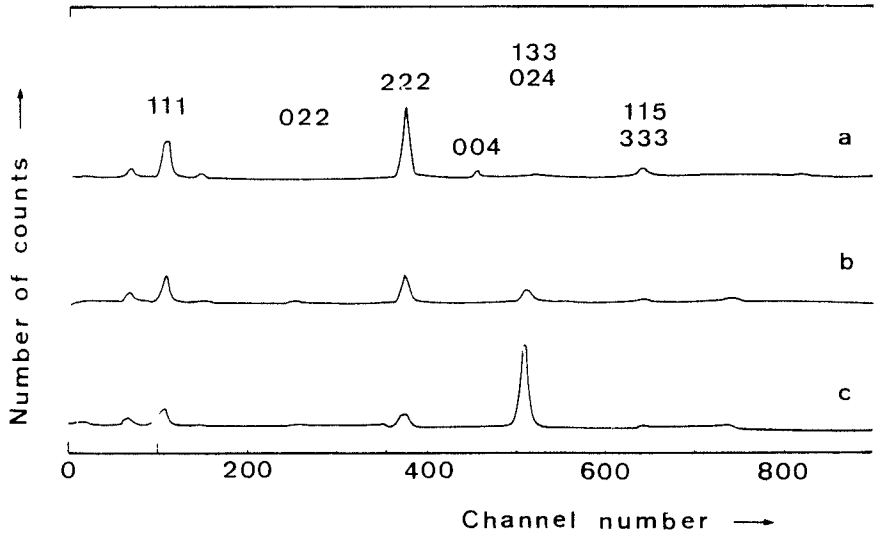


FIGURE 8. Energy-dispersive X-ray diffraction patterns recorded at different stages of the deformation of an aluminium wire. $2\theta_0 \approx 30°$. (a) Load 4.0 kg. (b) Load 5.1 kg. (c) Load 6.5 kg. Notice the changes in texture. Break occurred at the load 10.5 kg.

support is gratefully acknowledged. The authors wish to thank Professors L. Lindegaard-Andersen and B. Buras for reading the manuscript and for valuable comments. They are also indebted to B. Ribe for technical assistance.

REFERENCES

1. B. C. Giessen and G. E. Gordon, *Science*, 159, 973 (1968).
2. B. Buras, J. Chwaszczewska, S. Szarras and Z. Szmid, Institute of Nuclear Research (Poland), Report No. 894/II/PS (1968).
3. E. Laine and I. Lähteenmäki, *J. Mater. Sci.*, 6, 1418 (1971).
4. J. Szpunar, M. Ojanen and E. Laine, *Z. Metallkde.*, 65, 221 (1974).
5. J. Szpunar, A. Olés, B. Buras, I. Sosnowska and A. Pietras, *Nucleonika*, 13, 1111 (1968).
6. B. Buras, J. Staun Olsen, L. Gerward, B. Selsmark and A. Lindegaard Andersen, *Acta Cryst.*, A31, 327 (1975).
7. B. Buras and L. Gerward, *ibid.*, A31, 372 (1975).
8. O. Alstrup, L. Gerward, B. Selsmark, B. Buras and J. Staun Olsen, *ibid.*, A31, S 234 (1975).

9. G. B. Harris, *Phil. Mag.*, 43, 113 (1952); see also C. S. Barrett and T. B. Massalski, *Structure of Metals*, 3rd ed., McGraw-Hill, New York (1966).
10. International Tables for X-Ray Crystallography, Vol. III (1962) and Vol. IV (1974), Kynoch Press, Birmingham.